Parasitol Res (2012) 110:901–911
DOI 10.1007/s00436-011-2574-2

ORIGINAL PAPER

Liver response of rabbits to *Eimeria coecicola* infections

Saleh Al-Quraishy · Mahmoud S. Metwaly · Mohamed A. Dkhil · Abdel-Azeem S. Abdel-Baki · Frank Wunderlich

Received: 15 July 2011 / Accepted: 26 July 2011 / Published online: 6 August 2011

Abstract Intestinal coccidiosis of rabbits induced by *E. coecicola* causes enormous economic losses in rabbit farms. Here, we investigate the effect of *E. coecicola* on the liver of the rabbit *Oryctolagus cuniculus*. On day 7 p.i., fecal expulsion of *E. coecicola* oocysts is maximal and rabbits have lost approximately 25% of their weight. The liver, though not targeted by parasites, exhibits several signs of moderate inflammations, i.e., inflammatory cellular infiltrations around the central vein, dilatated blood sinusoids, increase in vacuolated hepatocytes, hypertrophic Kupffer cells, and lipid peroxidation as well as decreases in catalase and superoxide dismutase activities. Liver injuries are also indicated by an increase in blood plasma, by an increase in liver enzymes such as alanine transaminase, aspartate transaminase, alkaline phosphatase, and gamma glutamyl transferase, and a decrease in total protein and albumin. Circulating neutrophils have increased from 61% on day 0 p.i. to 71.3% on day 7 p.i., while lymphocytes are decreased from 37% to 26%. Agilent two-color oligo microarray technology, in combination with quantitative PCR, reveals that the expressions of 56 genes are upregulated and that of 22 genes are downregulated in the liver. The genes are largely involved in metabolism, calcium homeostasis, transport, and diverse signaling processes in the liver. In addition, numerous genes encoding for different regions of T-cell receptor as well as IgM, IgG, and IgA antibodies are both up- and downregulated in the liver by *E. coecicola* infections. The latter data suggest that the liver is not only 'passively' inflamed by intestinal infections with *E. coecicola* but rather is actively involved in the host defense against the intestinal *Eimeria* parasites.

S. Al-Quraishy · M. S. Metwaly · M. A. Dkhil (✉) · A.-A. S. Abdel-Baki · F. Wunderlich
Department of Zoology, College of Science,
King Saud University,
PO Box 2455, Riyadh 11451, Saudi Arabia
e-mail: mohameddkhil@yahoo.com

M. A. Dkhil
Department of Zoology and Entomology, Faculty of Science,
Helwan University,
Helwan, Egypt

A.-A. S. Abdel-Baki
Department of Zoology, Faculty of Science, Beni-Suef University,
Beni-Suef, Egypt

Introduction

Rabbit production has been greatly increased as a source of protein in recent years and has become one of the important animal resources in different countries including India and Saudi Arabia (Bhat et al. 1996; Al-Mathal 2008). However, this production is threatened by diseases, e.g., as intestinal coccidiosis, which cause severe diarrhea, weight depression, as well as mucoid bloody feces due to intestinal lesions (Peeters et al. 1984; Bhat and Jithendran 1995; Jithendran and Bhat 1996), and increased malnutrition due to disturbance of food absorbance and digestion (Baker 2007; Taylor et al. 2007), which finally lead to death and huge economic losses in industrial rabbit farms (Bhat et al. 1996).

The infectious agents of coccidiosis are parasitic protozoans belonging to the genus *Eimeria*. Among the 800 known *Eimerian* species (Mehlhorn 2008), there are 11 species specific for rabbits, including *Eimeria coecicola* (Bhat et al. 1996; Pakandl 2009). The life cycle of *E. coecicola* is characterized by the extraintestinal migration of the sporozoites, which appear to be essential to complete a life cycle (Pakandl et al. 1993, 1996; Renaux et al. 2001).

The final target sites of *E. coecicola*, however, are the cecum and the appendix, respectively. Incidentally, these intestinal parts are also targeted in the hosts by other *Eimerian* species such as *Eimeria tenella* (Mehlhorn et al. 1984; López-Bernad et al. 1998; Aarthi et al. 2010; DePablos et al. 2010).

The appendix tissue infected with *E. coecicola* has been described to undergo a series of structural changes (Vitovec and Pakandl 1989; El-Shahawi et al. 2011), which have been largely ascribed to the inflammatory response of the host. Recently, however, we have found in *Eimeria papillata* infections of mice that the inflammatory response of the host is not only confined to the final target site of the intestine (Dkhil et al. 2011a). By contrast, there is an even more pronounced response in the liver, though the liver is not a direct target site of *E. papillata* (Dkhil et al. 2011b). On the other hand, some information is available that microbial and food antigens derived from the intestine can reach the liver through the hepatic portal system and can elucidate inflammatory and immune responses in the liver (Nagura and Sumi 1988). For instance, there is an activation of Kupffer cells and natural killer cells, acute phase proteins, complement components, and cytokines as, e.g., IL-12 and IL-18 required for the Th-1 immune response in the liver (Seki et al. 2000).

In intestinal coccidiosis caused by *E. coecicola* infections, however, the liver of rabbits has not yet been investigated to date. This prompted us to characterize the response of the liver to *E. coecicola*, in particular at the level of gene expression using the Agilent two-color oligo microarray technology in combination with quantitative RT-PCR.

Materials and methods

Animals

Healthy female rabbits (*Oryctolagus cuniculus*), approximately 8–9 weeks old and ranging in weight from 2.0 to 2.5 kg, were obtained from the animal facilities of King Saud University. The animals were individually caged and were kept under constant conditions for at least 1 week before use. Their feces were examined daily during this week to assure the absence of any coccidial infection. The experiments were approved by the state authorities and followed the Saudi Arabian law on animal protection.

E. coecicola infections

Oocysts of *E. coecicola* of rabbit appendix (Pakandl 1989) for later experimental infections were collected from feces of rabbits naturally infected with *E. coecicola* and then surface-sterilized with sodium hypochlorite and washed at least four times in sterile saline as described by Schito et al. (1996). These oocysts were used to inoculate rabbits by oral gavaging of each rabbit at a dose of 50,000 sporulated oocysts (Pakandl et al. 1993) suspended in 1 ml sterile saline. Once every 24 h at 2 p.m., fresh feces were collected and each rabbit was weighted. Oocyst output was measured as previously described (Schito et al. 1996). In brief, fecal pellets were suspended in 2.5% (wt/vol) potassium dichromate and diluted in saturated sodium chloride for oocyst flotation. Oocysts were counted using a modified Mcmaster technique (Georgi 1980) and expressed as the number of oocysts per gram of feces.

Sample collection

Six infected and six non-infected rabbits were killed and dissected on day 7 p.i. Blood was taken from the heart into heparinized tubes for the determination of hematological parameters and the other part was used to obtain plasma for biochemical studies. Plasma was stored at −80°C until use. Liver was removed and cut into small pieces in sterile saline. Some pieces were kept in sterile tubes under liquid nitrogen, other pieces were fixed in neutral buffered formalin for histological studies, and other pieces were suspended in Tris buffer for biochemical studies.

Histology and immunohistochemistry

Formaline-fixed pieces of the liver were dehydrated and embedded in paraffin, and 5-μm-thick sections were stained with eosin–hematoxylin. For immunohistochemical localization of Kupffer cells, paraffin sections were cleared in xylene, rehydrated in graded ethanol solutions (100–70%), immersed in water for 5 to 10 min, and incubated in 0.3% H_2O_2/70% methanol for 20 min to inhibit endogenous peroxidase activity. The specimens were then rinsed in PBS three times for 5 min, and epitopes were unmasked by boiling in citrate buffer (pH 6.0) for 10 to 15 min, if necessary. Sections were blocked for 30 to 60 min in 3% bovine serum albumin (BSA) dissolved in PBS or in 5% goat or rabbit serum in PBS and were incubated with anti-CD68 primary antibody in PBS-buffered 0.1% BSA overnight at 4°C in a humidified chamber. The samples were then rinsed in PBS and incubated with 7.5 g/ml of the biotinylated secondary antibody in PBS-buffered 0.1% BSA for 1 h at room temperature, followed by avidin/biotin amplification (ABC Elite) for 30 min, before developing with 3,3-diaminobenzidine peroxidase substrate. Sections were counterstained with Mayer hematoxylin for 2 to 5 min. Negative controls were performed with PBS instead of the primary antibody (Huang et al. 2010).

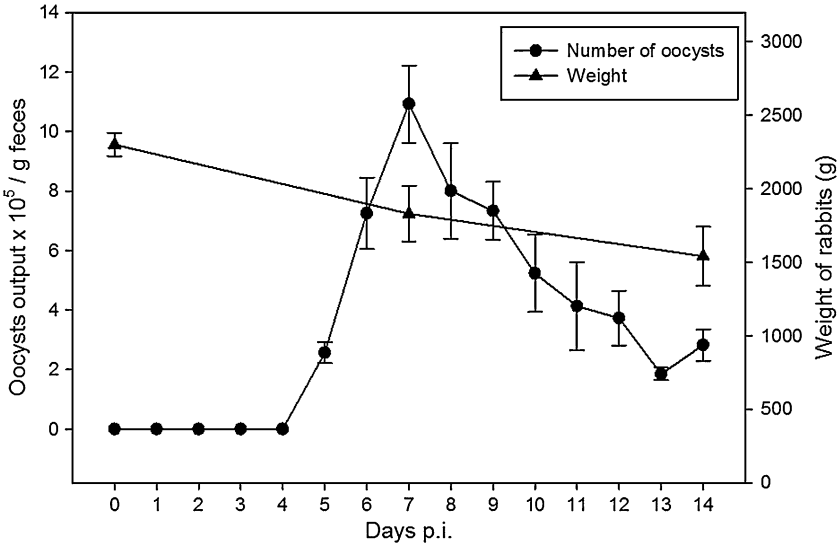

Fig. 1 Course of *E. coecicola* infections in rabbits. Rabbits were infected with sporulated oocysts on day 0 and the fecal outputs of oocysts as well as the weight of rabbits were followed during 14 days. Values represent means ± SD (n=6)

Hematology

Samples were analyzed using Vet abc™ Animal Blood Counter (Horiba ABX, Montpellier, France) using hematology kits specified for that instrument (Horiba ABX, France).

Biochemical determinations

Plasma was analyzed using commercial kits (Biomerieux, Marcy l'Etoil, France) for alanine aminotransferase (ALT) (Bergmeyer 1985), aspartate aminotransferase (AST) (Bergmeyer 1985), gamma glutamyltransferase (GGT) (Szasz 1969), alkaline phosphatase (ALP) (Epstein et al. 1986), and total bilirubin (TB) (Walters and Gerarde 1970) according to the instructions of the manufacturers. Oxidative stress markers were determined in liver homogenates using commercial kits (Biodiagnostic, Dokki, Giza, Egypt) for catalase (Aebi 1984), superoxide dismutase (Nishikimi et al. 1972), and malondialdehyde (Satoh 1978) according to the manufacturer's instructions. Using commercial kits (Biomerieux, Marcy l'Etoil, France), plasma was assayed for glucose (Trinder 1969), albumin (Walsh 1983), total lipids (Knight 1972), total cholesterol (Trinder 1969), and triglycerides (Fossati and Principe 1982). Absorbance was measured using the Ultrospec 2000 U/V spectrophotometer (Amersham, Pharmacia Biotech, Cambridge, England).

RNA isolation

Trizol was used to isolate total RNA (Sigma-Aldrich), the quality and integrity of which were determined using the Agilent RNA 6000 Nano Kit on the Agilent 2100 Bioanalyzer (Agilent Technologies). RNA was quantified by measuring A_{260nm} on the ND-1000 Spectrophotometer (NanoDrop Technologies, Wilmington, NC, USA).

Amplification and labeling of RNA

Labeling was performed as detailed in the 2-Colour Microarray-Based Gene Expression Analysis protocol (version 5.5, part number G4140-90050). In brief, 1 μg of total RNA samples was amplified and labeled with cyanine 3-CTP and cyanine 5-CTP (Perkin Elmer, Waltham, MA, USA). Yields of cRNA and the dye incorporation were measured with the ND-1000 Spectrophotometer.

Hybridization of Agilent Whole Rabbit Genome Oligo Microarrays

Hybridization was performed according to the two-color microarray-based gene expression analysis protocol (version 5.5, part number G4140-90050) using the Agilent Gene Expression Hybridization Kit (Agilent Technologies, Palo Alto, CA, USA). Briefly, 825 ng of the corresponding Cy3- and Cy5-labeled cRNA were combined and hybridized overnight (17 h at 65°C) to Agilent Whole Rabbit Genome Oligo Microarrays 4×44 containing 43,603 gene-specific rabbit oligo spots by using Agilent's recommended

Table 1 Changes in liver function biomarkers in the blood plasma of rabbits infected with *E. coecicola*

Parameter	Day 0	Day 7
ALT (U/L)	54.7±13	38±4
AST (U/L)	41±5.3	50.2±3.3[a]
ALP (U/L)	92.6±12.7	144.8±33.6
GGT (U/L)	5.5±2.1	12.1±1.2[a]
Bilirubin (mg/dl)	0.7±0.3	0.3±0.1

Values are means ± SD

[a] Significant change at $p \leq 0.01$

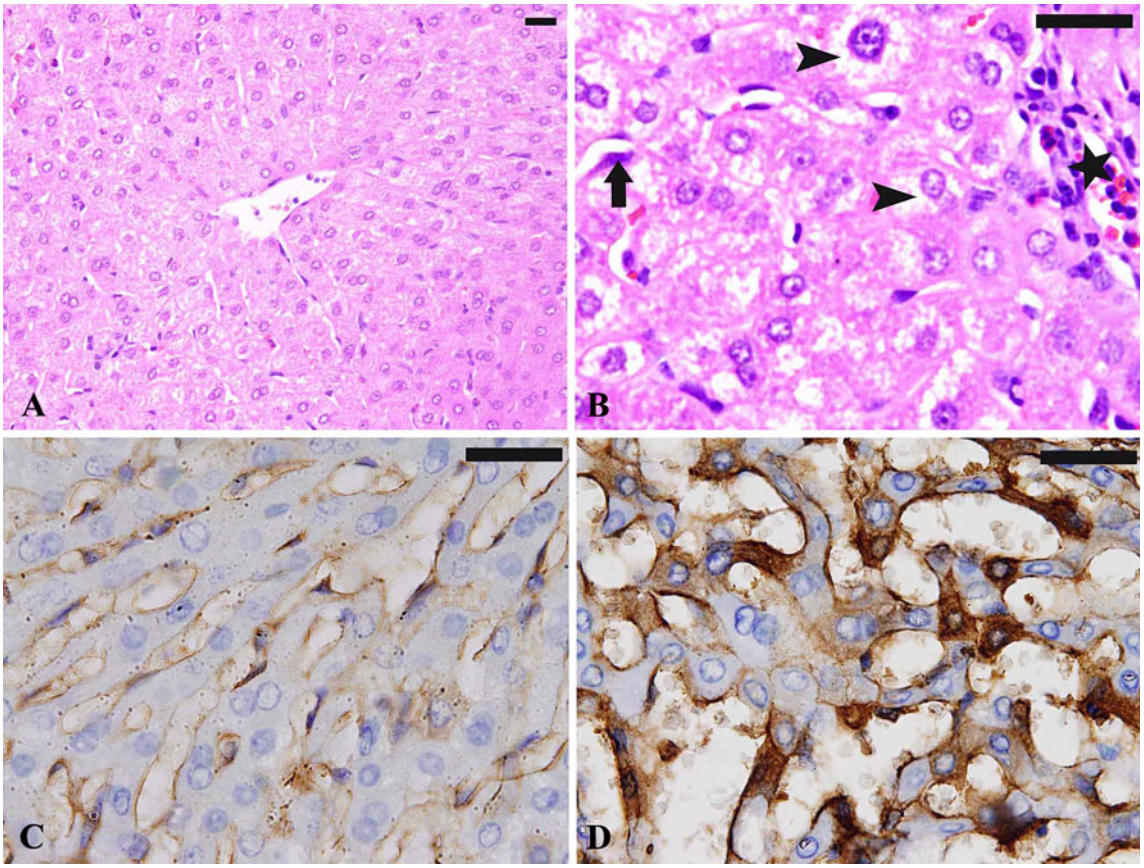

Fig. 2 Effect of *E. coecicola* infections on liver tissue on day 7 p.i. Eosin/hematoxylin- stained liver sections of non-infected control rabbits (**a**) and infected rabbits (**b**). Liver sections labeled with the Kupffer cell detecting anti-CD68 antibody in non-infected (**c**) and infected rabbits (**d**). *Arrow* indicates Kupffer cell; *arrowhead* indicates vacuolated hepatocytes. *Bar* indicates 25 μm

hybridization chamber and oven. The microarrays were then washed once with 6x SSPE buffer containing 0.005% *N*-lauroylsarcosine for 1 min at room temperature before washing with preheated 0.06x SSPE buffer at 37°C containing 0.005% *N*-lauroylsarcosine for 1 min. The last washing step was performed with acetonitrile for 30 s.

Table 2 Systemic changes in rabbits infected with *E. coecicola*

Parameter	Day 0	Day 7
Neutrophils (%)	61±2.0	71.3±2.1[a]
Lymphocytes (%)	37±2.8	26±1.4[a]
Glucose (mg/dl)	121.2±8	143.8±7.1[a]
Albumin (g/dl)	4.6±0.4	4.3±0.3
Globulin (g/dl)	2.7±0.3	2.1±0.1[a]
Urea (mg/dl)	14.4±1.	25.7±1.1[a]
Total lipids (mg/dl)	254.7±30.3	454.3±77.2[a]
Total cholesterol (mg/dl)	32.9±3.7	66.9±12[a]
Triglycerides (mg/dl)	44.5±6.7	184.4±21.5[a]
Uric acid (mg/dl)	1.8±0.4	0.6±0.1[a]

Values are means ± SD

[a] Significant change at $p \leq 0.01$

Scanning and data analysis

The fluorescence signals of the hybridized Agilent microarrays were detected with the Agilent's Microarray Scanner System G2505B and the Scan Control Software (Agilent Technologies, Palo Alto, CA, USA). The Agilent Feature Extraction Software (FES) version 10.2.1.3 was used to read out and process the microarray image files. Differential gene expression of the FES-derived output data files were determined by the Rosetta Resolver® gene expression data analysis system (Rosetta Biosoftware). To this end, the local signal of each spot was measured inside a 300-μm-diameter

Table 3 Oxidative stress biomarkers in liver of rabbits infected with *E. coecicola*

Days p.i.	Malondialdehyde (nmol/g)	Catalase (u/g)	Superoxide dismutase (u/g)
0	171.9±25.9	7.7±0	13,306±1,798
7	308.9±34.3[a]	5.8±0.4[a]	5,953±1,663[a]

Values are mean ± SD

[a] Significant change at $p \leq 0.01$

Table 4 Upregulated genes in the liver of *O. cuniculus* infected with *E. coecicola* on day 7 p.i.

Gene symbol	Gene name	Fold change Inf/C	Agilent ID	Representative public ID	GO ID	Functions
Immune response						
GZMH	Granzyme H	13.10	A_04_P032776	EF472898		Serine protease that is expressed by cytotoxic immune cells
SAA1	Serum amyloid protein A 1	10.30	A_04_P000796	NM_001082327	0002526, 0006953	Acute phase response and acute inflammatory response
SAA2	Serum amyloid protein A 2	8.60	A_04_P004476	NM_001082392	0002526, 0006953	Acute phase response and acute inflammatory response
SAA3	Serum amyloid protein A 3	8.50	A_04_P000811	NM_001082302	0002526, 0006953	Acute phase response and acute inflammatory response
CR1	CR1 complement component (3b/4b) receptor (knops blood group)	7.40	A_04_P033564	EU407475		Negative regulator of the complement cascade
IL2	Interleukin 2	5.40	A_04_P003997	AF068057	0050863, 0050864	Regulation of B and T cell activation, TH1/TH2 differentiation
CRP	C-reactive protein, pentraxin-related	4.80	A_04_P003657	NM_001082265	0002526, 0006953	Acute phase response and acute inflammatory response
TAC1	Tachykinin, precursor 1	4.60	A_04_P004753	NM_001101698	0007217, 0006953	Tachykinin receptor signaling pathway, inflammatory response
ORM1	Orosomucoid 1	4.20	A_04_P001646	NM_001101695	0002526, 0006953	Acute phase response and acute inflammatory response
IL4	Interleukin 4	3.70	A_04_P004866	AF169169	0050863, 0050864	Regulation of B and T cell activation, TH1/TH2 differentiation
LBP	Lipopolysaccharide binding protein	3.60	A_04_P013032	M35534	0002526, 0006953	Acute phase response and acute inflammatory response
MRP-8	Macrophage migration inhibitory factor-related protein-8	3.30	A_04_P013129	D17405		Involved in chemotaxis of neutrophils and monocytes
HP	Haptoglobin	3.20	A_04_P003271	NM_001082110	0002526, 0006953	Acute phase response and acute inflammatory response
HPX	Hemopexin	2.90	A_04_P003321	NM.001082760	0002526, 0006953	Acute phase response and acute inflammatory response
TRF	Liver transferrin	2.80	A_04_P001611	NM_001101694	0002526, 0006953	Acute phase response and acute inflammatory response
RLA-DMB	Histocompatibility antigen DM heterodimer light chain-like	2.60	A_04_P013506	U77896		MHC class II molecule
Metabolism						
CA4	Carbonic anhydrase IV	15.10	A_04_P001796	NM_001082372	0006730	One-carbon metabolic process
LOC100144327	Xanthine dehydrogenase/ oxidase	6.90	A_04_P001056	NM_001122938	0055114	Involved in purine metabolism
CYP19A1	Cytochrome P450, family 19, subfamily 1, polypeptide 1	6.40	A_04_P013086	Z70301	0055114	Phase I metanbolism
APOA1	Apolipoprotein A-I	6.00	A_04_P001491	NM_001101687	0006869, 0008203	Lipid transport, cholesterol metabolic process
ACE	Angiotensin-converting enzyme (peptidyl-dipeptidase A) 1	3.90	A_04_P002340	NM_001082395		Involved in blood pressure control
ADAM2	ADAM2 metallopeptidase	2.60	A_04_P001193	NM_001082677	0006508, 0007155	Involved in proteolysis and cell adhesion
CYP2E1l	Cytochrome P450 2E1-like	2.50	A_04_P012584	M15061	0055114	Phase I metabolism
Calcium						
SLN	Sarcolipin	8.60	A_04_P003030	NM_001082387	0051924	Regulation of calcium ion transport
CASQ1	Calsequestrin 1	5.40	A_04_P001204	NM_001082268	0005509	Calcium ion binding
CASQ2	Calsequestrin 2	4.70	A_04_P001543	NM_001101691	0005509	Calcium ion binding
LOC100008703	Calgranulin C	2.80	A_04_P013462	AF091848		Involved in calcium signaling
PRKCB	Protein kinase C, beta	2.60	A_04_P001742	NM_001101723		Calcium signaling
Transporter						
SLC26A3	Solute carrier 2family 6, member 3	20.90	A_04_P000772	NM_001082098	0008272	Sulfate transport
SLC22A2	Solute carrier family 22 (organic cation transporter), member 2	5.30	A_04_P000583	NM_001082115	0006811	Organic anion transport
PAT1	Proton/amino acid transporter 1	4.90	A_04_P002494	NM_001082183	0016021	Symport of protons and small neutral amino acids such as glcine, alanine and proline
KCNK1	Potassium channel, subfamily K, member 1	4.20	A_04_P003133	NM_001082180	0006813	Potassium ion transport
SLC2A1	Solute carrier family 2 (facilitated glucose transporter), member 1	3.30	A_04_P000624	NM_001105687	0008643	Carbohydrate transport

Table 4 (continued)

Gene symbol	Gene name	Fold change Inf/C	Agilent ID	Representative public ID	GO ID	Functions
SLC6A8	Solute carrier family 6 (neurotransmitter transporter, creatine), member 8	3.20	A_04_P001381	NM_001082397	0006836	Neurotransmitter transport
CLCNKA	Chloride channel	3.10	A_04_P000411	NM_001082361	0006821	Chloride transport
KCNB2	Potassium voltage-gated channel, Shab-related subfamily, member 2	2.90	A_04_P001853	NM_001082137	0006813	Potassium ion transport
ATP1A2	ATPase, Na/K transporting, alpha 2 polypeptide	2.80	A_04_P016156	AF235025	0006874	Cellular calcium ion homeostasis
Signaling						
SPP1	Secreted phosphoprotein	22.50	A_04_P000146	NM_001082194	0007155	Involved in cell adhesion
PTGER3	Prostaglandin E receptor 3 (subtype EP3)	16.90	A_04_P000446	NM_001082671	0007186	G-protein receptor protein signaling pathway
RLN1	Relaxin1	12.90	A_04_P003442	NM_001082320	0005179	Hormone activity
CGA	Glycoprotein hormones, alpha polypeptide	5.20	A_04_P003182	NM_001082724	0006590	Involved in thyroid hormone generation
KGF	Keratinocyte growth factor	4.50	A_04_P063732	AF049241		Induces epithelialization during wound healing
PHKA1	Phosphorylase kinase alpha subunit	3.70	A_04_P013222	M64656	0005977	Glycogen metabolism
MT3	Metallothionein 3	3.3	A_04_P101902	NM_001082220	0045596	Negative regulation of cell differentiation
DMBT1	Deleted in malignant brain tumors 1	3.10	A_04_P002461	NM_001082033	0005044	Scavenger receptor activity
PRLR	Prolactin receptor	3.00	A_04_P013497	Z83759	0060644, 0060736	Involved in mammary gland and prostate gland differentiation
Miscellaneous						
TINAG	Tubulointestinal nephritis antigen	18.00	A_04_P001237	NM_001082786	0006508	Involved in protein degradation
LOC100009510	Small intestinal receptor adhesion molecule	13.30	A_04_P016496	AY894815		Unknown
MUC1	Mucin 1, cell surface associated	7.50	A_04_P014136	U85787		Binds to pathogens, overexpression often associated with colon cancer
LPXN	Leupaxin	4.40	A_04_P001881	NM_001082048		Cell adhesion protein
FAM23A	Family with sequence similarity 23, member A-like	3.90	A_04_P082375	NM_001101709	0016021	Integral to membrane
COL10A1	Collagen type X	3.10	A_04_P016280	AY598937	0031012	Extracellular matrix
EEF1A2	Eukaryotic translation elongation factor 1 alpha 2	3.10	A_04_P002506	NM_001082031	0006414	Involved in translational elongation
ZAN	Zonadhesin	3.10	A_04_P001244	NM_001082081	0007155	Cell adhesion
MG72/JP1	Mitsugumin72/junctophilin type 1	2.60	A_04_P000807	NM_001081996	0007517	Muscle organ development
VCAN	Versican	2.60	A_04_P013241	AF020293		

Inf infected rabbits; *C* non-infected control rabbits

circle and the local background was determined within 40-μm-wide rings approximately 40 μm distantly from the signal and subtracted from the local signal intensity to calculate the net signal intensity and the ratio of Cy5 to Cy3. The ratios were normalized to the median of all ratios, considering only those spots with fluorescence intensities three times larger than that of the herring sperm DNA and spotting buffer negative controls. The values represent the means of four single spots with their standard deviations.

Quantitative real-time PCR

Total RNA was digested by DNAse using the DNA free kit (Ambion) to remove any contaminating genomic DNA. Then, he QuantiTect Reverse Transcription kit (Qiagen) was used to synthesize cDNA. Amplifications were performed in TaqMan7500 (Applied Biosystems) using Quanti Tect SYBR Green PCR kit (Qiagen) and gene-specific Quanti Tect primer assays (Qiagen) according to the manufacturer's instructions. Following an initial incubation at 50°C for 2 min, Taq polymerase was activated by incubation at 95°C for 10 min. During the following 55 cycles made up of 15 s at 95°C, 35 s at 60°C, and 30 s at 72°C, the amount of double-stranded PCR product was measured as SYBR green fluorescence at the end of the extension phase. All PCR reactions yielded only a single product species of the expected size as revealed by melting point analysis and gel electrophoresis. Relative quantitative evaluation of amplification data was done using Taqman7500 system software v.1.2.3f2 (Applied Biosystems).

Statistical analysis

Student's *t* test was used to determine significant differences.

Results

All the six rabbits, when infected with the intestinal parasite *E. coecicola*, begin to shed oocysts with their feces on day 5 p.i. (Fig. 1). Maximal shedding of approximately 1.1 million oocysts per gram of feces of rabbit occurs on approximately day 7 p.i. Concomitantly, the average weight of rabbits decreases by approximately 25%. This weight loss is associated with watery mucoid diarrhea, lethargy, and decreased uptake of water and food. At maximal shedding of oocysts on day 7 p.i., most hematological parameters such as hemoglobin concentration, number of red blood cell and platelets, packed cell volume, mean corpuscular hemoglobin, and mean corpuscular hemoglobin content are not significantly changed (data not shown). Only the neutrophils increase from 61± 0.7% on day 0 p.i. to 71.3±2.1% on day 7 p.i., while lymphocytes decrease from 37±2.8% to 26±1.4%, respectively. Moreover, there is a significant increase in glucose, urea, total lipids, total cholesterol, and triglycerides (Table 1).

The liver of *E. coecicola*-infected rabbits macroscopically appears somewhat enlarged and darkened in color on day 7 p.i. A microscopic examination of eosin/hematoxylin-stained liver sections did not reveal any parasites (Fig. 2). Nevertheless, the liver has undergone some moderate pathological changes such as inflammatory cellular infiltrations, hepatocytic vacuolations, sinusoid dilatations, and edematous hepatocytes in comparison to livers of non-infected rabbits

Table 5 Downregulated genes in the liver of *O. cuniculus* infected with *E. coecicola* on day 7 p.i.

Gene symbol	Gene name	Fold change Inf/C	Agilent ID	Representative public ID	GO ID	Functions
Immune response						
CD1B	CD1b molecule	−2.57	A_04_P002276	NM_001089312	0019882	Antigen processing and presentation
CCL2	Chemokine (C-C motif) ligand 2	−2.60	A_04_P001371	NM_001082294	0006854, 0006935	Inflammatory response, chemotaxis
ADAM17	Tumor necrosis factor-alpha-converting enzyme	−2.74	A_04_P032702	EF472913		Involved in the cleavage and release of the soluble ectodomain from membrane-bound pro-TNFα
IL8	Interleukin 8	−2.80	A_04_P004968	NM_001082293	0006854, 0006935, 0030155	Inflammatory response, chemotaxis, regulation of cell adhesion
IL1A	Interleukin1, alpha	−2.84	A_04_P002091	NM_001101684	0002526, 0006953	Acute phase response and acute inflammatory response
Metabolism						
FMO3	Flavin containing monooxygenase 3	−2.52	A_04_P003447	NM_001082246	0055114, 0031227	Phase I metabolism, intrinsic to endoplasmic reticulum membrane
CYP2C4l	Cytochrome P450 2C4-like	−2.59	A_04_P029832	J02716	0055114	Phase I metabolism
MME	Membrane metallo-endopeptidase	−2.63	A_04_P001473	NM_001101685	0006508	Involved in proteolysis
SULT1C4	Sulfotransferase family, cytosolic, 1C, member 4	−2.79	A_04_P000126	NM_001082711	0016782	Phase II metabolism, transferring sulfur-containing groups, cytosolic
CYP2C1l	Cytochrome P450 2C1-like	−3.00	A_04_P012572	K01522	0055114	Phase I metabolism
CYP2A11	Cytochrome P450 2A11	−3.40	A_04_P012756	L10237	0055114	Phase I metabolism
ACE-1	Acetylcholinesterase	−3.43	A_04_P012961	U05036	0001505	Regulation of neurotransmitter levels
GNMT	Glycine *N*-methyltransferase	−5.33	A_04_P102807	D13307	0042278, 0046500	Involved in purine and S-adenosylmethionine metabolism
DIO1	Deionidase, iodothyronine, type 1	−8.40	A_04_P001656	NM_001099958	0004800	Throxine 5′deionidase activity, thyroid hormone biosynthesis
Calcium						
SRL	Sarcolumenin	−2.95	A_04_P000304	NM_001082281	0005509	Calcium ion binding in sarcoplasmic reticulum
FKBP1B	FK506 binding protein 1B, 12.6 kDa	−3.15	A_04_P002342	NM_001082145	0006874	Cellular calcium ion homeostasis
CACB	Calcium channel	−3.26	A_04_P000025	X55763	0006816	Calcium ion transport
Miscellaneous						
CCND1	Cyclin D1	−2.51	A_04_P029937	DQ845180	0000082, 0000077	G1/S transition of mitotic cell cycle; DNA-damage checkpoint, p53 signaling pathway
SPOT14	Thyroid hormone-responsive protein	−2.54	A_04_P032677	EF428024		Thyroid hormone inducible hepatic SPOT14
MX-2	Interferon inducible protein Mx-2	−2.58	A_04_P013516	AB016251		GTPase activity
CSN1S2A	Alpha-S2-casein-like A	−2.97	A_04_P002552	NM_001082400	0005576	Secreted in extracellular region
SGCG	Sarcoglycan, gamma	−3.03	A_04_P001173	NM_001082362	0007010	Cytoskeleton organization

(Fig. 2a, b). In particular, a pronounced hyperplasia of Kupffer cells can be recognized with anti CD-68 antibody immunohistochemical stain (Fig. 2c, d). There also occur changes in liver functions as indicated by a significant increase in plasma activities of the liver enzymes AST, ALP, and GGT (Table 2). Moreover, infections with *E. coecicola* induce changes of oxidative stress biomarkers in hepatic tissue (Table 3). The activities of the antioxidant enzymes catalase and superoxide dismutase were decreased in the liver, whereas lipid

Table 6 Up- and downregulated genes encoding diverse regions of antibodies in the liver of rabbits infected with *E. coecicola* on day 7 p.i.

Gene name	Fold change Inf/C	Agilent ID	Representative public ID
Ig H-chain V-region (allotype VHa1) mRNA (V-D-J), clone RVH135	7.4	A_04_P012641	M21263
Clone mp137VL antibody variable domain, partial cds	5.4	A_04_P014826	AY171891
Rearranged IgH heavy-chain mRNA, VDJ region, allotype VHa2	5.3	A_04_P012717	M77055
Rearranged IgH heavy-chain mRNA, VDJ region, allotype VHa2	4.1	A_04_P012717	M77060
Clone DL5761 IgM heavy-chain VDJ region mRNA, partial cds	3.8	A_04_P031483	AF264589
IgA-alpha heavy-chain constant region mRNA fragment	2.5	A_04_P016571	X00353
Clone mp151VL antibody variable domain, partial cds	−2.5	A_04_P015846	AY175470
Clone mp067VH antibody variable domain, partial cds	−2.5	A_04_P015483	AY171750
Clone P20 immunoglobulin mu heavy chain VDJ region	−2.5	A_04_P029740	AF014694
Clone mp122VL antibody variable domain, partial cds	−2.6	A_04_P014772	AY171861
Clone mp146VH antibody variable domain, partial cds	−2.6	A_04_P015823	AY171907
Rabbit (clone 4 G18-IgG) IG rearranged H-chain V-D-J regions	−2.6	A_04_P012897	M99534
Clone mp180VH antibody variable domain	−2.6	A_04_P015964	AY175527
Rabbit Ig H-chain V-region (latent allotype VHa1) (V-D-J), clone RVH622	−2.5	A_04_P012662	M21272
Clone mp047VH antibody variable domain, partial cds	−2.5	A_04_P015415	AY171710
Clone mp087VL antibody variable domain	−2.7	A_04_P014636	AY171791
Rabbit (Clone 4 G19-IgG) IG rearranged H-chain V-D-J regions	−2.7	A_04_P012904	M99538
Clone mp078VL antibody variable domain	−2.7	A_04_P029502	AY171773
Clone mp099VL antibody variable domain	−2.8	A_04_P014681	AY171815
Clone KJ5733 IgM heavy chain VDJ region	−2.8	A_04_P013816	AF264557
clone mp019VL antibody variable domain	−2.9	A_04_P029542	AY171656
Rabbit Ig lambda chain V-J-C region, 3′ end, clone pDH101	−2.9	A_04_P031642	M25618
Clone 2307 IgM heavy chain VDJ region	−2.9	A_04_P014304	AF029932
Clone mp061VL antibody variable domain	−3	A_04_P014456	AY171739
Clone P206 immunoglobulin mu heavy chain VDJ region	−3	A_04_P013360	AF014728
Clone mp076VL antibody variable domain	−3	A_04_P015536	AY171769
Clone mp081VL antibody variable domain	−3.1	A_04_P014611	AY171779
Clone mp074VL antibody variable domain	−3.1	A_04_P015516	AY171765
Clone mp088VH antibody variable domain	−3.4	A_04_P015597	AY171792
Anti-human A33 immunoglobulin light chain variable region	−3.4	A_04_P013696	AF245500
Clone mp062VL antibody variable domain	−3.8	A_04_P014391	AY171741
Clone DL5554 IgM heavy chain VDJ region	−4	A_04_P033372	AF264578
Clone mp134VL antibody variable domain	−4.7	A_04_P014811	AY171885
Clone mp109VL antibody variable domain	−4.9	A_04_P014731	AY171835
Clone mp089VL antibody variable domain	−5.4	A_04_P014646	AY171795
Rabbit Ig kappa light chain (bas) V-J-C	−5.5	A_04_P012751	K01280
Clone DL6244 IgM heavy chain VDJ region	−5.6	A_04_P013795	AF264490
CD1b molecule	−5.8	A_04_P002276	NM_001089312
Clone mp205VH antibody variable domain	−5.9	A_04_P016032	AY175577
Clone mp007VL antibody variable domain	−6	A_04_P014396	AY171632
Clone mp196VH antibody variable domain	−6.3	A_04_P029401	AY175559
Clone mp022VL antibody variable domain	−6.6	A_04_P014451	AY171662

peroxidation was increased as indicated by a significant rise of malondialdehyde (Table 3).

In order to analyze any possible changes in hepatic gene expression induced by *E. coecicola* infections, we have compared the gene expression profiles between non-infected and infected rabbits on day 7 p.i. Using Agilent two-color microarray technology, numerous hepatic genes with altered expression profiles were found. In the following we describe only those genes whose expression has changed more than 2.5-fold, which was highly significant ($p \leq 0.01$). There were 56 genes upregulated and 22 genes downregulated, which we have categorized into several groups (Tables 4 and 5). The genes deregulated by *E. coecicola* infections can be summarized to be largely involved in metabolism, calcium homeostasis, transport, and signaling processes of the liver. Remarkably, however, most changes were observed in those genes which can be ascribed to be involved in the immune response. The upregulations of genes range between 2.5- and 22.5-fold, while downregulations vary between −2.5 to −5.3-fold (Tables 4 and 5).

A total of 16 genes were especially upregulated, which include not only those encoding for acute phase proteins such as SAA1-3, CRP, and transferrin but also those for the T-cell receptor (Table 4). In addition, only the five genes encoding CD1-β, CCL2, ADAM 17, IL-8, and IL-1α were downregulated (Table 5). Remarkably, there is a significant number of upregulated genes encoding for diverse regions of IgM, IgG, and IgA antibodies, whereas only a few of such genes are downregulated (Table 6). The microarray data can be at least partly verified by quantitative PCR. Figure 3 shows that the expression profiles of some genes arbitrarily selected from microarray analysis closely resemble those expressions determined by quantitative PCR.

Discussion

The final target site of *E. coecicola* is known to be the intestine, especially the appendix (Bhat et al. 1996; Pakandl et al. 1996, 2006). However, the route of migration and penetration of the intestine by sporozoites is rather complex (Pakandl et al. 2006). Indeed it appears as if an extra-intestinal migration of the parasite through mesenteric lymph nodes and spleen is an integral part of the early life cycle of the majority of the sporozoites before invading and intracellularly developing in different parts of the intestine and finally in cecum and appendix, respectively (Pakandl et al. 2006; Pakandl 2009).

The present study indicates that the oral infection of the rabbit *O. cuniculus* with *E. coecicola* sporulated oocysts leads to the final intracellular development of the parasites in the intestine. Indeed the beginning of the fecal output of *E. coecicola* oocysts is observed on day 5 p.i., and maximal shedding is reached on day 7 p.i. Also, *E. coecicola* parasites do not target the liver on day 7 p.i., though the liver strongly responds to *E. coecicola* infections. Indeed there are a number of structural signs of moderate inflammations in the liver coinciding with oxidative tissue damage as indicated by the increased lipid peroxidation and decreased activities of catalase and superoxide dismutase. In addition, injuries of the liver are also reflected by the increased release of the liver enzymes AST, ALP, and GGT. In this context, it is noteworthy that rabbits suffering from hepatic coccidiosis caused by *Eimeria stiedae* have also been previously reported to exhibit increases in serum AST and ALT activities, depending on the state of hepatocellular damage (San Martín-Núñez et al. 1988), and in serum activities of GGT due to cholestasis (Hein and Laemmler 1978). The present results also support our previous data

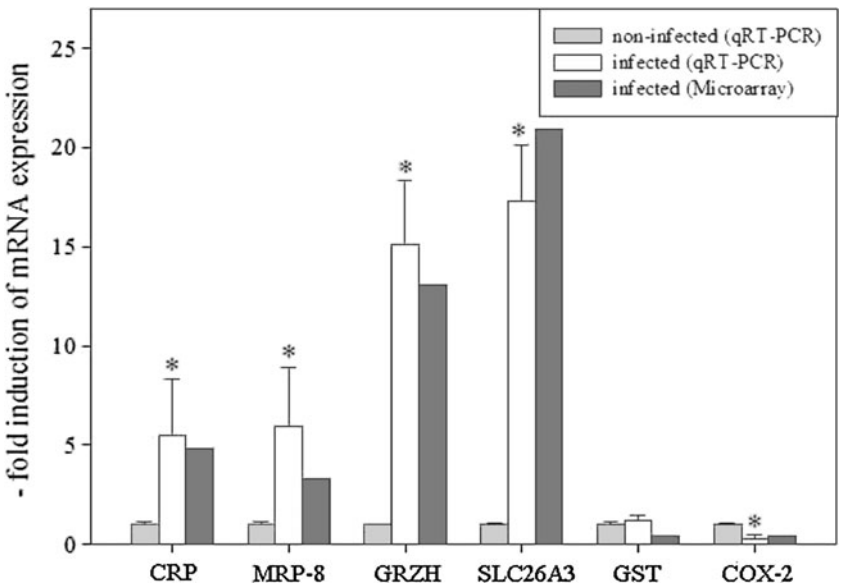

Fig. 3 Verification of liver gene expression by quantitative real-time PCR of genes arbitrarily selected from oligo microarrays obtained from the liver of non-infected rabbits and rabbits infected with *E. coecicola* on day 7 p.i. *Stars* indicate significant differences between infected and non-infected control animals. *CRP* C-reactive protein, *MRP-8* macrophage migration inhibitory factor protein 8, *GRZH* Granzyme H, *SLC26A3* solute carrier family 26A3, *GST* glutathione-*S*-transferase, *COX-2* cyclo oxygenase 2 enzyme

showing that another species of *Eimeria*, namely, *E. papillata*, which exclusively targets the jejunal part of the intestine in the mouse, also injures the liver of most mice, though the liver is not a target site of *E. papillata* (Dkhil et al. 2011b). Indeed the alterations found in the liver of mice infected with *E. papillta* at maximal fecal shedding of oocysts resemble those changes described here for the liver of *E. coecicola*-infected rabbits.

In extension of the previous *E. papillata* study, we have here detected profound liver changes at the level of gene expression induced by *E. coecicola* infections on day 7 p.i. The microarray analysis reveal that *E. coecicola* infections affect the expression of genes involved in metabolism, transport, Ca^{2+} homeostasis, and signaling processes in the liver. However, the majority of genes deregulated by *E. coecicola* can be ascribed to be involved in the immune response. Indeed genes encoding proteins belonging to innate and adaptive immunity are both up- and down-regulated in the liver by *E. coecicola* infections. For instance, the expression of genes encoding acute phase proteins such as SAA1-3, CRP, and transferrin were upregulated. Surprising, however, is the fact that genes encoding T-cell receptors and diverse regions of IgM, IgG, and IgA antibodies were also up- and downregulated. In this context, it has to be emphasized that the liver is also a lymphoid organ (Häussinger et al. 2004; Crispe 2009) and contains both intrahepatic T cells and B cells besides migratory circulating T and B cells. The changes we observe in hepatic gene expression may be therefore due to both intrahepatic and migratory T and B cells. For instance, upregulation may reflect both increased synthesis of specific mRNAs in intrahepatic T and B cells as well as increased immigration of T and B cells from the circulation to the liver. Conversely, downregulations may be indicative of decreased synthesis and increased emigration of these cells from the liver, respectively.

The liver is a first-pass organ as the intestine, and both are directly connected through the portal vein (Seki et al. 2000; Häussinger et al. 2004). The liver can be directly affected by *E. stiedae* which is known to infect the gall bladder (Toulah and AL-Rawi 2007). However, *E. coecicola* affects the liver indirectly. It is possible that inflammatory mediators induced by *E. coecicola* in the intestine are passively transferred to the liver, in which they induce inflammation, antigen presentation, and activation of specific T and B cells, respectively. However, it appears more likely that there is a close and coordinate cooperation between intestine and liver in the host defense against *E. coecicola* infections, i.e., *E. coecicola* antigens directionally move to the liver, initiating specific immune mechanisms, and hepatic T and B cells in turn may help in the final resolution of *E. coecicola* infections in the intestine and appendix, respectively. However, it cannot be definitely excluded that the response of the liver to *E. coecicola* infections is primed by early sporozoites, which apparently require an early extraintestinal route, though the liver has not yet been reported to be invaded by *E. coecicola* sporozoites (Pakandl 2009).

Collectively, our data indicate that intestinal infections with *E. coecicola* cause inflammatory and specific immune reactions in the liver, though the latter is not a direct target site of *E. coecicola*. Possibly, the liver immune reactions assist the host defense against the intestine stages of the parasites, thus contributing eventually to the resolution of intestinal *E. coecicola* infections. Future work is required to investigate these mechanisms in more detail and to extend this view to other intestinal *Eimeria* species in rabbits and other hosts as, e.g., *E. papillata* infections in mice (Dkhil et al. 2011a, b).

Acknowledgment The authors appreciate the Deanship of Scientific Research at King Saud University for funding this work through research group project no. RGP-VPP-002.

References

Aarthi S, Dhinakar Raj G, Raman M, Gomathinayagam S, Kumanan K (2010) Molecular prevalence and preponderance of *Eimeria* spp. among chickens in Tamil Nadu, India. Parasitol Res 107:1013–1017

Aebi HU (ed) (1984) Catalase. In: Methods in enzymatic analysis. Academic, New York, pp 276–86

Al-Mathal EM (2008) Hepatic coccidiosis of the domestic rabbit *Oryctolagus cuniculus domesticus* L. in Saudi Arabia. World J Zool 3:30–35

Baker DG (2007) In: Flynn's parasitology of laboratory animals, 2nd edn. Blackwell, Ames, p 840

Bergmeyer HU (1985) Approved recommendation on IFCC method for the measurement of catalytic concentration of enzymes, part 3. IFCC method for alanine amino transferase. Clin Chem Clin Biochem J 24:481–495

Bhat TK, Jithendran KP (1995) *Eimeria magna*: the effect of varying inoculum size on the course of infection in Angora rabbits. World Rabbit Sci J 3:163–166

Bhat TK, Jithendran KP, Kurade NP (1996) Rabbit coccidiosis and its control: a review. World Rabbit Sci J 4:37–41

Crispe IN (2009) The liver as lymphoid organ. Ann Rev Immunol 27:147–163

DePablos LM, dos Santos MF, Montero E, Garcia-Granados A, Parra A, Osuna A (2010) Anticoccidial activity of maslinic acid against infection with *Eimeria tenella* in chickens. Parasitol Res 107:601–604

Dkhil M, Addel-Baki A, Delic D, Wunderlich F, Sies H, Al-Quraishy S (2011a) *Eimeria papillata*: upregulation of specific miRNA-species in the mouse jejunum. Exp Parasitol 127:581–586

Dkhil MA, Abdel-Baki AS, Wunderlich F, Sies H, Al-Quraishi S (2011b) Anticoccidial and antiinflammatory activity of garlic in murine *Eimeria papillata* infections. Vet Parasitol 175:66–72

El-Shahawi GA, El-Fayomi HM, Abdel-Haleem HM (2011) Coccidiosis of domestic rabbit (*Oryctolagus cuniculus*) in Egypt: light microscopic study. Parasitol Res, in press

Epstein E, Kichle FL, Artiss JD (1986) The clinical uses of alkaline phosphatase enzyme. Clin Lab Med 6:491–505

Fossati P, Principe L (1982) Serum triglycerides determined colorimetrically with an enzyme that produces hydrogen peroxide. Clin Chem 28:2077–2080

Georgi JR (1980) Parasitology for veterinarians, 3rd edn. Saunders, Philadelphia, p 179

Häussinger D, Kubitz R, Reinehr R, Bode JG, Schliess F (2004) Molecular aspects of medicine: from experimental to clinical hepatology. Mol Asp Med 25:221–360

Hein B, Laemmler G (1978) Alteration of enzyme activities in serum of *Eimeria stiedae* infected rabbits. Parasitol Res 57:199–211

Huang W, Metlakunta A, Dedousis N, Zhang P, Sipula I, Dube JJ, Scott DK, O'Doherty RM (2010) Depletion of liver Kupffer cells prevents the development of diet-induced hepatic steatosis and insulin resistance. Diabetes 59:347–357

Jithendran KP, Bhat KP (1996) Subclinical coccidiosis in Angora rabbits—a field survey in Himachal Pradesh (India). World Rabbit Sci 4:29–32

Knight JA (1972) Chemical basis of sulfophospho-vanillin reaction in estimating total lipids. Clin Chem 18:199–204

López-Bernad F, del Cacho E, Gallego M, Quílez J, Sánchez-Acedo C (1998) Immunohistochemical identification of the cells parasitized by second-generation schizonts of *Eimeria tenella*. Parasitol Res 84:132–135

Mehlhorn H (ed) (2008) Encyclopedic reference of parasitology, vol 1, 3rd edn. Springer, Berlin

Mehlhorn H, Ortmann-Falkenstein G, Haberkorn A (1984) The effects of sym. triazinones on developmental stages of *Eimeria tenella*, *E. maxima* and *E. acervulina*: a light and electron microscopical study. Parasitol Res 70:173–182

Nagura H, Sumi Y (1988) Immunological functions of the gut, role of the mucosal immune system. Toxicol Pathol 16:154–164

Nishikimi M, Rao A, Yagi K (1972) The occurrence of superoxide anion in the reaction of reduced phenazinemethosulphate and molecular oxygen. Biochem Biophys Res Commun 46:849–854

Pakandl M (1989) Life cycle of *Eimeria coecicola* Cheissin, 1947. Folia Parasitol (Praha) 36:97–105

Pakandl M (2009) Coccidia of rabbit: a review. Folia Parasitol (Praha) 56:153–166

Pakandl M, Coudret P, Licois D (1993) Migration of sporozoites and merogony of *Eimeria coecicola* in gut-associated lymphoid tissue. Parasitol Res 79:593–598

Pakandl M, Gaca A, Drout-Viard F, Coudret P (1996) *Eimeria coecicola* Cheissin, 1947: endogenous development in gut-associated lymphoid tissue. Parasitol Res 82:347–351

Pakandl M, Sewald B, Drouet-Viard F (2006) Invasion of the intestinal tract by sporozoites of *Eimeria coecicola* and *Eimeria intestinalis* in naive and immune rabbits. Parasitol Res 98:310–316

Peeters BE, Charlier G, Antoine O, Mammericlex M (1984) Clinical and pathological changes after *Eimeria intestinalis* infection in rabbits. J Vet Med 31:9–24

Renaux S, Viard FD, Chanteloup NK, Vern Y, Kerboeuf D, Pakandl M, Coudret P (2001) Tissues and cells involved in the invasion of rabbit intestinal tract by sporozoites of *Eimeria coecicola*. Parasitol Res 87:98–106

San Martín-Núñez BV, Ordóñez-Escudero D, Alunda JM (1988) Preventive treatment of rabbit coccidiosis with alpha-difluoromethylornithine. Vet Parasitol 30:1–10

Satoh K (1978) Serum lipid peroxide in cerebrovascular disorders determined by a new colorimetric method. Clin Chem Acta 90:37–43

Schito ML, Barta JR, Chobotar B (1996) Comparison of four murine *Eimeria* species in immunocompetent and immunodeficient mice. J Parasitol 82:255–262

Seki S, Habu Y, Kawamura T, Takeda K, Dobashi H, Ohkawa T, Hiraide H (2000) The liver as crucial organ in the first line of host defense: the roles of Kupffer cells, natural killer (NK) cells and NK1.1 Ag^+ T cell in T helper 1 immune responses. Immunol Rev 174:35–46

Szasz G (1969) A kinetic photometric method for serum gamma glutamyltranspeptidase. Clin Chem 15:124–136

Taylor MA, Coop RL, Wall RL (2007) Veterinary parasitology, 3rd edn. Blackwell, Ames, p 901

Toulah FH, AL-Rawi MM (2007) Efficacy of garlic extract on hepatic coccidiosis in infected rabbits (*Oryctolagus cuniculus*): histological and biochemical studies. J Egypt Soc Parasitol 37:957–969

Trinder P (1969) Determination of glucose in blood using glucose oxidase with an alternative oxygen acceptor. Ann Clin Biochem 6:24–28

Vitovec J, Pakandl M (1989) The pathogenicity of rabbit coccidium *Eimeria coecicola* Cheissin, 1947. Folia Parasitol 36:289–293

Walsh RL (1983) A comparison of dye-binding methods for albumin determination; the effects of abnormal sera, reaction times, acute phase reactants and albumin standards. Clin Biochem 16:178–181

Walters MA, Gerarde HW (1970) An ultramicro method for the determination of conjugated and total bilirubin in serum or plasma. Microchemistry 15:231–243